Nanomed. J. 5(4): 227-234, Autumn 2018

RESEARCH PAPER

# Mathematically and experimentally defined porous bone scaffold produced for bone substitute application

*Hamed Joneidi Yekta [1], Maryam Shahali [2], Siros Khorshidi [1], Soheila Rezaei [3], Amir Hussein Montazeran [1], Saeed Saber Samandari [1], David Ogbemudia [4], Amirsalar Khandan [*1]*

[1]*New Technologies Research Center, Amirkabir University of Technology, Tehran 15875-4413, Iran*
[2]*Department of Quality Control, Research and Production Complex, Pasteur Institute of Iran, Tehran, Iran*
[3]*Department of Molecular Genetic, National Institute of Genetic Engineering and Biotechnology, Tehran, Iran*
[4]*Mechanical Engineering Department, Eastern Mediterranean University, North Cyprus, Gazimağusa, TRNC, Mersin 10, Turkey*

## ABSTRACT

***Objective (s):*** Artificial bone implants have been studied as a possible bone replacement for fractured and destroyed facial tissue; the techniques employed to determine the success of the dental implants. The stability, porosity and resistance of the bone implant which is subjected to varying forces and stresses within the surrounding bone is a subject of interest among the dentists.

***Materials and Methods:*** An experimental analysis was conducted on bio-nanocomposite scaffold using space holder methods. The reaction of the bio-nanocomposites deformation under load was determined using Abaqus software. Thereafter, an analytical solution was presented to express explicitly the deformation responses of the artificial bone implant.

***Results:*** It was observed that the vibrational behavior and mechanical performance of the sample containing 15 wt% additives has shown better mechanical characteristic compared to the pure specimen. On the other hand, the additive weight fraction has a significant effect on the compression test and porosity value. Also, the elastic modulus of the samples increases more than two times with the addition of additive (from 60 MPa to 145 MPa). From the results, it can be concluded that the highest vibration variation is seen in the sample with lower MNPs percentages.

***Conclusion:*** By observing the results of the stresses, it was observed that level of stress was a small value in bio-nanocomposites with highest amount of reinforcement.

***Keywords:*** *Abaqus, Nanocomposite, Porous bone implant, Scaffold, Stress analysis*

**How to cite this article**

*Joneidi Yekta H, Shahali M, Khorshidi S, Rezaei S, Montazeran AH, Saber-Samandari S, Ogbemudia D, Khandan AS. Mathematically and experimentally defined porous bone scaffold produced for bone substitute application. Nanomed J. 2018; 5(4): 227-234. DOI: 10.22038/nmj.2018.05.00007*

## INTRODUCTION

The bone is a living, growing, and important tissue in the human body. Therefore, like other living parts, it requires nutrients, oxygen, heat and pressure to thrive. Bone has the incredible ability to repair itself, and function as a structural skeleton that hold the body together [1-4]. The outer part of the rigid bone is made of the organic substance such as collagen and mineral substance such as calcium phosphate (CaPs) and calcium carbonate (CaC) [5-7]. In addition to playing the role of mechanical support to the organs, the bone is responsible for the storage of minerals (especially $Ca^{2+}$ and $PO_4^{2-}$) [8-13]. According to literature, the osteoporosis or dissolution of the inner part of the bone leads to relatively low mechanical properties (such as compressive strength and fracture toughness) in an aqueous medium like blood and water [14-18]. Therefore, for application purposes, the second phase of composites are incorporated into the hydroxyapatite (HA) phase and need to be investigated by researchers. Also, special types of reinforcement's materials were developed to enhance mechanical properties of CaPs called synthetic non-toxic magnetite

* *Corresponding Author Email: sas.khandan@aut.ac.ir*
Note. This manuscript was submitted on August 5, 2018; approved on September 1, 2018

nanoparticle (MNPs). Young's modulus of dense HA bioceramics changed with respect to the porosity and impurities values [18, 30]. Moreover, this substance exhibited superplastic properties at high temperature i.e. about 1000°C to 1100°C. The fracture toughness of HA ceramic material also declines linearly as the porosity increased [19-23]. Recently, new generation of bioceramics were developed called calcium silicate (CS) including diopside, clay, akermanite, baghdadite, and bredigite [13, 24-28]. Also, the results showed that akermanite was able to form apatite in a Simulated Body Fluid (SBF) better than diopside products. The MTT assay confirmed the biosynthesis and proliferation of human bone marrow stem cells (BMSC) in contact with akermanite. The results of the MTT test confirmed the non toxicity of akermanite ceramics [28-32]. The porosity of the bone increased over time as the bone grew higher. For example, the flexural strength of porous implant is about 40-60 MPa. Moreover, this allows the manufacturing process to be controlled with a high degree of control over the particle size, morphology and porosity [18-21]. The finite element analysis (FEA) can perform exceptionally well in predicting bone mechanism and mechanical forces response. The FEA can be used for testing bone implant before surgery, scaffold design, and structural tissue engineering. As a general principle, the ideal scaffolds for tissue repair should be non-toxic, have good biocompatibility, and be biodegradable (be compatible with the cells regarding to have proper porosity). Therefore, to predict the mechanical performance of the bio-nanocomposites, we produced akermanite-magnetite scaffold bio-nanocomposite using space holder technique and NaCl particles as spacer type. The purpose of this study is to investigate the numerical and experimental analysis of the bone architecture, which made of magnetite scaffold bio-nanocomposite. Thereafter, an analytical solution was presented to express explicitly the load-frequency and frequency-deflection responses of the bone beam-type implant using axial compressive strength and initial mechanical properties from the experimental tests. The influence of the MNPs weight fraction on the natural vibrational of the bio-nanocomposite implant was investigated using Abaqus software.

## *MATERIALS AND METHODS*

### *Materials preparation*

In this study, a silicate calcium powder (Akermanite: AK) powder and magnetite nanoparticles (MNPs) were synthesized using high energy ball milling (HEBM) and co-precipitation technique. The ball to powder weight ratio (BPR) was taken as 15:1, the rotational speed of 650 rpm, and $N_2$ gas were used according to the previous research [32, 38]. The akermanite and MNPs were milled using HEBM process for 1 hour with 0, 5, 10, and 15 wt% MNPs nanopowder. The nanocomposites powder were added with 65-70 wt% sodium chloride (NaCl) particle with spacer size less than 10-20 (μm) (Merck Company, purity 98%). The obtained homogeneous nanocomposite mixture was pressed using pressing machine (SANTAM STM-50, New Technology Research Centre, Amirkabir University of Technology) with applied force about of 120-160 MPa in a cubic die for 50-65 second as shown in Fig 1. Subsequently, in order to create AK-MNPs scaffolds via the space holder method, the appropriate weight ratio of the prepared composite nanopowder together with 65-70 wt% amount of NaCl particles are put

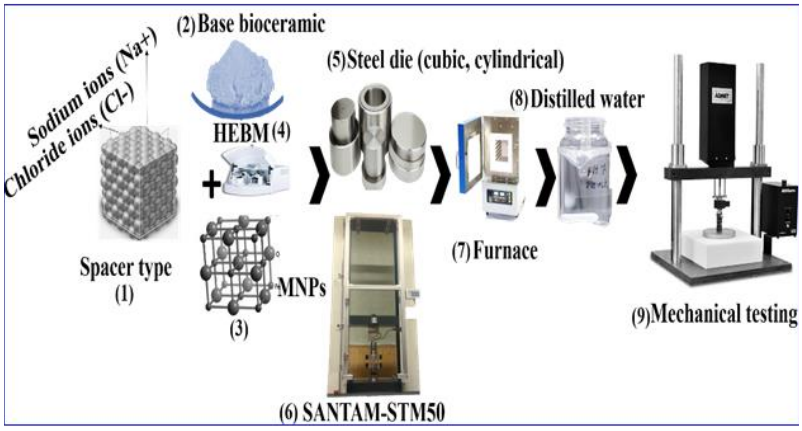


Fig 1. Schematic of preparation of AK-MNPs bio-nanocomposite scaffold using space holder technique

to use.

The powders were weighted and pressed in a cubic steel mold (using 1 gr sunflower oil), with dimensions of the sample size (14×15×6 $mm^3$). After that, the samples were sintered in the furnace at 1100°C for 60 min. The remained NaCl particles were eliminated by immersing the block samples in deionized water for 24 hours at room temperature as shown in Schematic Fig 1.

***Testing materials***

***Compressive strength evaluation***

The compressive strength of the AK-MNPs bio-nanocomposite scaffolds was performed using SANTAM machine. The crosshead speed of 2 mm/min for the prepared samples with various amounts of MNPs powder. The elastic modulus of the fractured sample was measured using the Hooke's equation. Also, the values of the elastic modulus calculated from the slope of the linear part of the stress-strain curve. The results are expressed in terms of a mean value accompanied by a standard deviation (SD=±3) and appropriate ASTM standard. Additionally, to measure the Poisson's ratios, the ratio of the total transverse elastic deformation of the bio-nanocomposite scaffolds to its axial elastic deformation were calculated as below formula: $\nu = -\varepsilon_y/\varepsilon_x$

Where $\varepsilon_y$ is the transverse strain resulting from the applied axial strain $\varepsilon_x$ in a 2D Cartesian coordinate system with an orthogonal x- and y-axes. Where  is the transverse strain resulting from the applied axial strain  in a 2D Cartesian coordinate system with an orthogonal x- and y-axes. The extracted date from the experimental

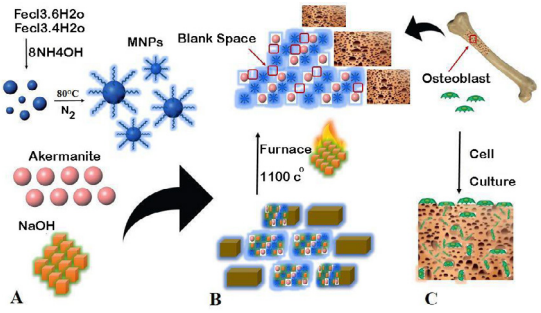


Fig 2. The process of preparation of AK-MNPs bio-nanocomposite scaffold for bone tissue engineering application, (A) sample preparation, (B) the scaffold fabrication technique, and (C) scaffolds cell attachment

procedure were inserted into Abaqus software to simulate the mechanical performance of the specimens. The samples were tested using scanning electron microscopy (SEM), particle size (PSA) and X-ray diffraction (XRD) analysis to evaluated the phase and morphological behavior of materials.

Fig (2-a) introduced the preparation of starting materials (AK and MNPs) for using in the current study. Fig (2-b) explained the fabrication procedure of the bio-nanocomposites scaffold using high temperature sintering process. Fig (2-c) shows the cell behavior and cell attachment on the scaffold surface after implantation. Ideally, a scaffold has the following characteristics like porous, bioactive, and biodegradable property. In addition, it possess adequate mechanical properties suited to the biological site. It has sufficient porosity, which is needed to accommodate cell proliferation and differentiation to enhance tissue formation. The bio-nanocomposite scaffold should have high interconnectivities between pores for uniform cell seeding and distribution, and for the nutrients and metabolites exchange at the cell/scaffold architecture. Another important characteristic of the scaffold allows the replacement of biological tissues via physiological extracellular components without leaving toxic degradation products as shown in Fig 2.

***Model using finite element analysis (FEA)***

The models that make up the exact geometry of the human bone can be obtained in a variety of methods using the Abaqus software jointly with scanners. The most common method for inserting an ideal organ into a computer environment is through the use of a scanner. However, for the living organs, radiographic images are more useful with the necessary processing applied on the scanned images. Due to the existing two-dimensional images and the final shape, it is important that the radiograph scans of the bone tissue in parallel or cross-sections represented similarly to Fig 2(c). On the other hand, when gridding and meshing for a Finite Element Model (FEM), as mentioned above, the four elements that are utilized can be applied with respect to the number of elements used later in the meshing process. Therefore, the number of triangles can be directly related to each other. Therefore, due to fact that the bone doesn't have direct contact with the force, it makes no sense to use a larger number of triangles to describe it, and it is better to introduce it by simplifying its

geometry. This can speed up the implementation used in the finite element program and ease up the modeling process. Regarding the focus of this article on the applied forces to the human artificial bone on the analysis of stress within the bone, due to various forces applied on the bone, it is assumed that the bone has been shown in the Ramus region as shown in Fig 2-c. Fig 4 showed that the toughness of the sample with a higher amount of MNPs was higher than the pure sample, measured the surface under stress-strain curve. For modeling the vibration behavior and the actual size of a bone model, the closed surfaces around it acts to determine the position and orientation of each of these triangular components by three points as shown in Fig 5 (a-c).

The findings from the Abaqus model showed that changes in cylindrical shape was caused by the vertical forces. These changes are made suddenly on bioceramics, leading to sudden fracture or fracture stress regarding their brittle feature. Therefore, the boundary condition of this problem was the nodes in the Ramus area i.e. where it was fixed. Therefore, it was decided that loading should be carried out in two ways, i.e. perpendicular and parallel orientation, with the direction of the lower bone.

## RESULTS AND DISCUSSION

XRD pattern of bio-nanocomposite scaffolds after sintering at 1100 °C for 60 min in the furnace shown on Fig 3. It is seen that the bio-nanocomposite containing magnetite nanoparticles

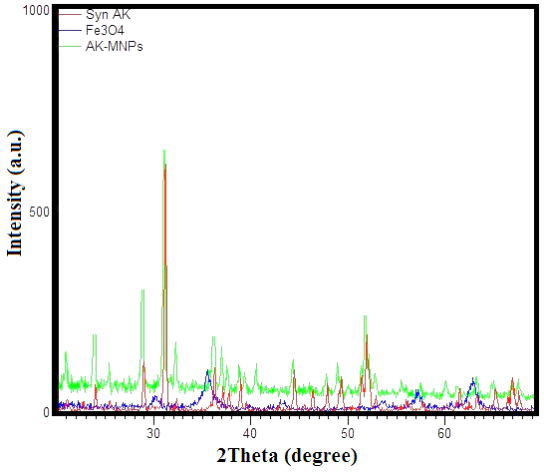


Fig 3. XRD pattern of the sample containing 15 wt% MNPs in bio-nanocomposite scaffold

contain sharp peaks which shift after sintering process. to the left side due to the milling process of the MNPs and AK powders. Fig 3 presents the phase characterization of the milled powders for several hours and sintered at 900°C. It is seen, there is no sign for any peak of starting and raw materials after sintering process.

The stress-strain curve for the samples at different weight fractions of (0, 5, 10, and 15 wt%) MNPs represented in Fig 4. The stress-strain curve indicated that sample with 15 wt% MNPs have highest yield strength and ultimate strength compared with the sample without MNPs scaffold. Recently, researchers composed MNPs with novel calcium silicate (type bredigite or hardystonite) for hyperthermia application under alternative current (AC) magnetic field with proper mechanical, magnetic behavior and biological response [19, 25, 29]. Yang et al. [33] investigated a new nanophase ceramic for enhanced drug carrier. It should be noted that the main part of the work is the design of the scaffold using space holder technique to produce architecture with proper porosity in the range of 70-85% beside adequate compressive strength [34-37], which is determined by the size of the cavity, bending properties, addition of magnetite nanoparticles, porosity and degree of degradability [38-42]. New types of bioceramics like nanoclay, akermanite, diopside, baghdadite, and bredigite were investigated as a reinforcement to CaPs and CS-based nanopowders to enhances their biomechanical, biological response and corrosion resistance in the physiological saline [43-44]. The resistance and mechanical stability of the scaffold to regional stresses and forces in the entire area of the scaffold is around 3-5 MPa. It is also clear that the sample without magnetic nanoparticles (with a greater weight ratio of akermanite) reduced the porosity value compared to the sample with a higher magnetite nanoparticles, and the porosity also decreased (on average), due to the increase in the weight ratio of the metalic phase. In addition the greater mechanical resistance of the scaffold walls that can be justified in the presence of remained salt during the sintering process. The bone must have proper elastic modulus and a high compression stress so that they can temporarily protect the texture mechanically, without any trace of fatigue or failure factor. One of the most important problems of orthopedic surgeons is the disconformity of bone hardness and metalic

implants and a large difference between the bone young modulus. At this stage, the properties of the

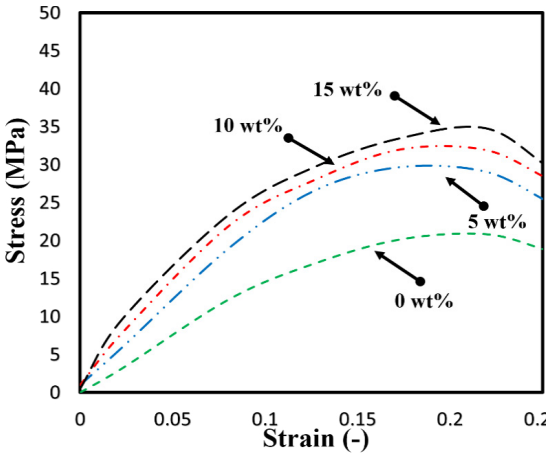


Fig 4. Stress-strain curve of the sample containing (0, 5, 10 , and 15 wt%) magnetite nanoparticle in akermanite nanocomposite scaffold

materials according to the analysis method, contact conditions between the components, loads and boundary conditions as well as the final segmentation of the cylindrical tissue is obtained. In this model, it is assumed that the implant completely connects to the bone and the osteogenic occurred. Li et al [45]. introduced a multi-scale modeling strategy to investigate the compressive strength performance of the carbon nanotube/polymer composites. Their model was proposed for the carbon nanotube (CNT) at the atomistic scale and the pattern deformation was examined by utilizing the continuum FEA technique. The interactions of the CNT atoms using van der Waals, which is used to analyze the behavior of carbon atoms with each other and the FE nodes of the matrix, were simulated using the truss rods [45-48]. To determine the Elastic Modulus of the interphase in the polymer nanocomposites, Saber-Samandari et al. [46, 49] stated that a three-dimensional cubic model can be used to describe the three component phases such as particle, interphase, and the matrix. Table 1 shows that with addition of MNPs to the base bioceramics the Elastic Modulus of the scaffolds increased which confirm the analytical results. Also, as the MNPs added to the based bioceramics the Poisson Ratio increases similar to the density value. Fig 5 shows the schematic of the sample containing 15 wt% MNPs in the (a) SANTAM-STM50 machine, (b) FEA model, and (c) the SEM images of the scaffold in the high stress part. Other changes observed in the stress-strain curve is the object's

Table 1. The values of Young's Modulus obtained via the experimental analysis for the bio-nanocomposite material with different MNPs weight fractions in the current study

| Materials | Density (g/cm$^3$) | Elastic Modulus (MPa) | Poisson Ratio |
|---|---|---|---|
| 0 wt % | 3.2 | 60±5 | 0.30 |
| 5 wt % | 3.5 | 85±5 | 0.30 |
| 10 wt % | 3.2 | 110±5 | 0.32 |
| 15 wt % | 3.3 | 145±5 | 0.34 |

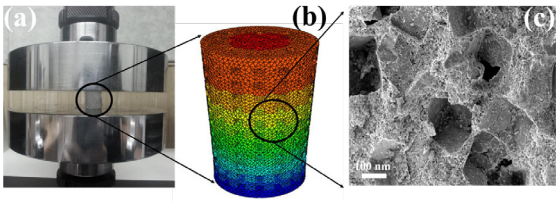


Fig 5. Schematic of the sample containing 15 wt% MNPs in the (a) Tensile test machine, (b) FEA model, and (c) the SEM images of the sample in the center of sample

resistance to permanent changes, which was made in the weld elastic region.

Restoration of the broken bones recently received the attention of biomaterials researchers using 3D printers in order to accelerate the process of broken bone repair. Scaffold materials are structures with three-dimensional tissue which direct the organization, growth, and differentiation of cells. Scaffolds must be biocompatible. They must be designed to meet both nutritional and biological needs for the specific cell population. Due to the importance of this component, today the three-dimensional structure of scaffolds is of great importance, and the designing is done by computers and special software. Due to the importance of this issue, it will be dealt with in detail in the next section. Growth factors are soluble peptides with the ability of binding cellular receptors and developing a permissive or preventive cellular response to tissue's differentiation and/or proliferation. ECM must be able to provide the optimal conditions for cell adhesion, growth, and differentiation within the construct through developing a system with the capability of controlling environmental factors including pH, temperature, oxygen tension, and mechanical forces. Bioreactors could be useful in improving and controlling the cell signaling. Different types of cells are employed in tissue engineering that can be classified in

several ways. In general terms, technologies in tissue engineering use both wholly differentiated progenitor cells at different steps of differentiation usually called “stem cells”. Stem cells are undifferentiated cells capable of dividing in culture and inducing different forms of specialized cells. The surface chemistry is also critical; cells and ECM molecules must contact with the scaffold surface through its surface molecules. According to the results, by increasing the power law, the natural frequency in cubic sheets with a metal-ceramic (magnetite nanoparticle-akermanite) decreases. The natural frequency of the cubic sheet is also reduced by increasing the side length in higher applied force. Finally, increasing the amount of non-uniformity also reduces the amount of natural frequency. Fig 6(a-c) shows the Von Misses Stress (VMS) analysis of the bio-nanocomposite scaffold, displacement analysis, and strain analysis of the bio-nanocomposite products with porous microstructure compared to the bulk sample. As it is seen the strain analysis and the VMS analysis of the sample with 15 wt% MNPs were similar to each other due to the similar maximum distortion energy criterion. The density, Elastic Modulus, Poisson ratio of the bio-nanocomposite scaffold were tabulate in Table 1. Also, the normal stress, average stress, ultimate stress, vibrational response, and the frequency of the samples are shown in Table 2. The red area showed a higher strain and stress in the cylindrical shape.

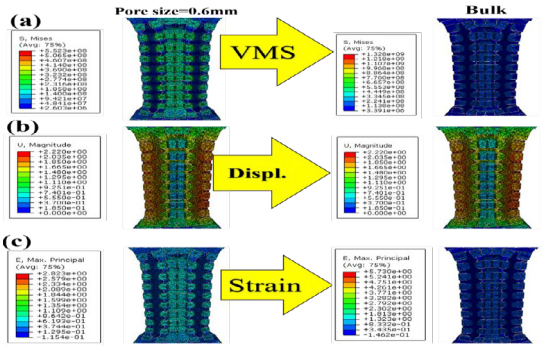


Fig 6. The (a) VMS, (b) displacement, and (c) the strain of the samples as pores and bulk sample with the Abaqus analysis

Table 2 shows the stress applied to the porous biomaterial scaffold in lateral and vertical direction. It shows that as the forces direction changes from vertical to lateral the normal stress, average stress, and the ultimate stress changes more than two times compared with the vertical direction. Also, it shows with porous size around 0.6 mm the stress parameters decreased to half times. The bio-nanocomposites was affected by a specific amount of force and finally, the shape of the object changed, even when the force was eliminated. As a result, the scaffold bio-nanocomposite did not return to its original state because of the elasticity of the ceramics. Another reason is that the deformation in the plastic region was permanent and not reversible as shown in Fig 6 (b-c).

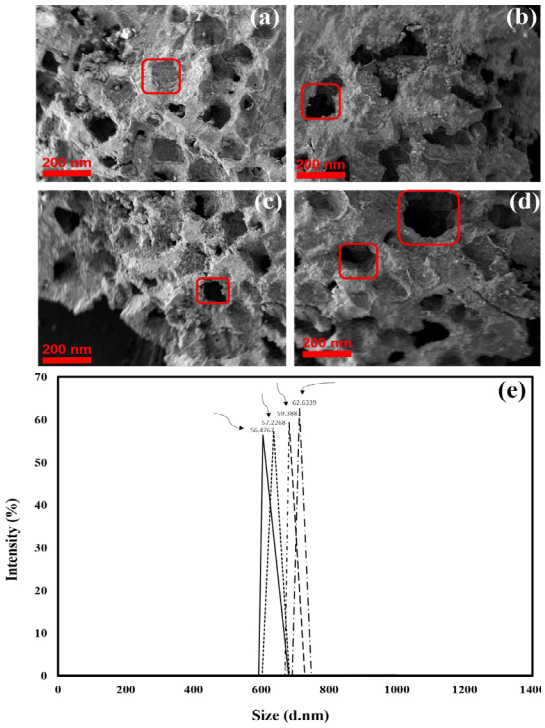


Fig 7. The SEM images specimen fabricated using space holder technique containing (a) 0 wt%, (b) 5 wt%, (c) 10 wt%, (d) 15 wt%, and (e) particle size analysis of magnetite nanoparticles bio-nanocomposite scaffold

The SEM images in Fig 7(a-d) shows that with addition of MNPs to the AK, the porosity of the scaffolds increased. The fracture toughness of scaffold material also declines linearly as the porosity increased. It is seen that addition of MNPs leads to creation of open porous interconnectivity hole, which is suitable for cell transition in the artificial bone. Fig 7(e) shows that increasing MNPs leads to an increasing in intensity of particle size of the bio-nanocomposite powders. The particle size analysis confirm the SEM results. Typical printers or technology to produce 3D design architecture has been used to create a suitable porous scaffold that can transmit the alive cells.

Table 2. The result of applied stress on the porous samples containing 15 wt% MNPs, Comparing fundamental frequency by considering various pore size (boundary condition: C-C)

| Materials | Normal stress | Average stress | Ultimate stress | Frequency (Hz) | Frequency (Hz) |
|---|---|---|---|---|---|
| Vertical force | 145 | 364 | 21000 | -- | -- |
| Lateral force | 268 | 582 | 40000 | -- | -- |
| 0.6 (mm) | 139.25 | 139.45 | 254.65 | 622.91 | 623.41 |

The inkjet printing method is capable of developing high resolution accurate designs. Studies have shown that the resolution of printed points in typical inkjet printers is about 25 to 30 ,which is similar to that of biological cells. In addition, it has been reported that under certain conditions, the inkjet system is capable of printing lines in the sub-micron range similar to space holder technique in the current study. To develop such a construct, a watchful selection of four key materials is needed: a) scaffold, b) growth factors, c) extracellular matrix, and d) cells.

## CONCLUSION

In this research, the new calcium silicate, akermanite bioceramic powder was synthesized using a high energy ball milling. Following this, the bio-nanocomposite powder made of akermanite and magnetite nanoparticles was compressed using a NaCl particle by employing the space holder technique, sintered at 1100 °C for 1 hr. The experimental analysis was then compared with the analytical results from the Abaqus software. The advantage of this technique was the sample's low cost and simplistic scaffold manufacturing process for bone tissue engineering. Additionally, the amount of positive stress was obtained and the FEA was effective in measuring and evaluating the highest force and distractive vibrational behavior. The obtained results indicated that the sample with 15 wt% MNPs has a better compressive strength and vibrational behavior responses. Also, the porosity of the samples was in the range of 75%-80%.

The maximum tension is related to the sample with the highest amount of MNPs, which also caused tightening of the torque. The natural frequency in cubic sheets with a metal-ceramic (magnetite nanoparticle-akermanite) structure decreases and also reduced by increasing the side length and higher applied force.

## ACKNOWLEDGMENTS

The authors would like to extend their gratitude for the support provided by the New Technology Research Centre, Tehran, and Iran.

## REFERENCES

1. Murugan R, Ramakrishna S. Development of nanocomposites for bone grafting. Comp Sci Tech. 2005; 65(15-16): 2385-2406.
2. Khandan A, Abdellahi M, Ozada N, Ghayour H. Study of the bioactivity, wettability and hardness behaviour of the bovine hydroxyapatite-diopside bio-nanocomposite coating. J Taiwan Inst Chem Eng. 2016; 60: 538-546.
3. Kazemi A, Abdellahi M, Khajeh-Sharafabadi A, Khandan A, Ozada N. Study of in vitro bioactivity and mechanical properties of diopside nano-bioceramic synthesized by a facile method using eggshell as raw material. Mater Sci Eng C. 2017; 71: 604-610.
4. Saber-Samandari S, Gross KA. Micromechanical properties of single crystal hydroxyapatite by nanoindentation. Acta Biomater. 2009; 5(6): 2206-2212.
5. Saber-Samandari S, Saber-Samandari S, Kiyazar S, Aghazadeh J, Sadeghi A. In vitro evaluation for apatite-forming ability of cellulose-based nanocomposite scaffolds for bone tissue engineering. Int J Biol Macromol. 2016; 86: 434-442.
6. Saber-Samandari S, Saber-Samandari S, Ghonjizade-Samani F, Aghazadeh J, Sadeghi A. Bioactivity evaluation of novel nanocomposite scaffolds for bone tissue engineering: The impact of hydroxyapatite. Ceram Int. 2016; 42(9): 11055-11062.
7. Khandan A, Karamian E, Bonakdarchian M. Mechanochemical synthesis evaluation of nanocrystalline bone-derived bioceramic powder using for bone tissue engineering. Dent Hypoth. 2014; 5(4): 155.
8. Saber Samandari S, Gross KA. Contact nanofatigue shows crack growth in amorphous calcium phosphate on Ti, Co-Cr and Stainless steel. Acta Biomater. 2013; 9(3): 5788-5794.
9. Saber Samandari S, Gross KA. Amorphous calcium phosphate offers improved crack resistance: A design feature from nature? Acta Biomater. 2011; 7(12): 4235-4241.
10. Saber-Samandari S, Gross KA. The use of thermal printing to control the properties of calcium phosphate deposits. Biomaterials. 2010; 31(25): 6386-6393.
11. Saber Samandari S, Alamara K, Saber-Samandari S. Calcium phosphate coatings: Morphology, micro-structure and mechanical properties. Ceram Int. 2014; 40: 563-572.
12. Sahmani S, Shahali M, Khandan A, Saber-Samandari S, Aghdam MM. (2018). Analytical and experimental analyses for mechanical and biological characteristics of novel nanoclay bio-nanocomposite scaffolds fabricated via space holder technique. Appl Clay Sci. 2018; 165: 112-123.
13. Razavi M, Khandan A. Safety, regulatory issues, long-term biotoxicity, and the processing environment. In Nanobiomat Sci Dev and Eval. 2017; 261-279.
14. Khandan A, Ozada N, Karamian E. Novel microstructure mechanical activated nano composites for tissue engineering applications. J Bioeng Biomed Sci. 2015; 5(1): 1.
15. Martin RB, Burr DB, Sharkey NA. Skeletal tissue mechanics. New York: Springer; 1998.
16. Qin QH. Mechanics of Cellular Bone Remodeling: Coupled Thermal, Electrical, and Mechanical Field Effects. CRC Press. 2013.
17. Zhang J, Wang Q, Wang A. In situ generation of sodium alginate/hydroxyapatite nanocomposite beads as drug-controlled release matrices. Acta Bimat. 2010; 6(2): 445-

454.
18. Dorozhkin SV. Calcium orthophosphate cements for biomedical application. J Mater Sci. 2008; 43(9): 3028.
19. Khandan A, Ozada N. Bredigite-Magnetite (Ca7MgSi4O16-Fe3O4) nanoparticles: A study on their magnetic properties. J Alloys Compd. 2017; 726: 729-736.
20. Abdellahi M, Karamian E, Najafinezhad A, Ranjabar F, Chami A, Khandan A. Diopside-magnetite; A novel nanocomposite for hyperthermia applications. J Mech Behav Biomed Mater. 2018; 77: 534-538.
21. Ghayour H, Abdellahi M, Ozada N, Jabbrzare S, Khandan A. Hyperthermia application of zinc doped nickel ferrite nanoparticles. J Phys Chem Solids. 2017; 111: 464-472.
22. Najafinezhad A, Abdellahi M, Saber-Samandari S, Ghayour H, Khandan A. Hydroxyapatite-M-type strontium hexaferrite: A new composite for hyperthermia applications. J Alloys Compd. 2018; 734: 290-300.
23. Abdellahi M, Najfinezhad A, Saber Samanadari S, Khandan A, Ghayour H. Zn and Zr co-doped M-type strontium hexaferrite: Synthesis, characterization and hyperthermia application. Chinese Journal of Physics. 2017: 28.
24. Ghayour H, Abdellahi M, Nejad MG, Khandan A, Saber-Samandari S. Study of the effect of the Zn2+content on the anisotropy and specific absorption rate of the cobalt ferrite: the application of Co1− xZnxFe2O4 ferrite for magnetic hyperthermia. J Aust Ceram Soc. 2017; 1-8.
25. Khandan A, Ozada N, Saber Samandari S, Nejad MG. On the mechanical and biological properties of bredigite-magnetite (Ca7MgSi4O16-Fe3O4) nanocomposite scaffolds. Ceram Int. 2018; 44(3): 3141-3148.
26. Mahmoudi K, Bouras A, Bozec D, Ivkov R, Hadjipanayis C. Magnetic hyperthermia therapy for the treatment of glioblastoma: a review of the therapy's history, efficacy, and application in humans. Int J Hyperthermia. 2018: 19: 1-36.
27. Karamian E, Abdellahi M, Khandan A, Abdellah S. Introducing the fluorine doped natural hydroxyapatite-titania nanobiocomposite ceramic. J Alloys Compd. 2016; 679: 375-383.
28. Khandan A, Jazayeri H, Fahmy MD, Razavi M. Hydrogels: Types, Structure, Properties, and Applications. Biomat Tiss Eng. 2017; 4: 143-169.
29. Sahmani S, Khandan A, Saber-Samandari S, Aghdam MM. Vibrations of beam-type implants made of 3D printed bredigite-magnetite bio-nanocomposite scaffolds under axial compression: Application, communication and simulation. Cer Int. 2018: 1; 44(10): 11282-11291.
30. Yang YC, Chang E, Lee SY. Mechanical properties and Young's modulus of plasma-sprayed hydroxyapatite coating on Ti substrate in simulated body fluid. J Biomed Mater Res. 2003; 67(3): 886-899.
31. Orlovskii VP, Komlev VS, Barinov SM. Hydroxyapatite and hydroxyapatite-based ceramics. Inorg Mater 2002; 38(10): 973-984.
32. Najafinezhad A, Abdellahi M, Ghayour H, Soheily A, Chami A, Khandan A. A comparative study on the synthesis mechanism, bioactivity and mechanical properties of three silicate bioceramics. Mater Sci Eng C. 2017; 72: 259-267.
33. Yang L, Sheldon BW, Webster TJ. Nanophase ceramics for improved drug delivery. Am Ceram Soc Bull. 2010; 24-32.
34. Sadeghzade S, Shamoradi F, Emadi R, Tavangarian F. Fabrication and characterization of baghdadite nanostructured scaffolds by space holder method. J Mech Behav Biomed. 2017; 68: 1-7.
35. Al-Attar AA, Zaeem MA, Ajeel SA, Latiff NE. Effects of SiC, SiO2 and CNTs nanoadditives on the properties of porous alumina-zirconia ceramics produced by a hybrid freeze casting-space holder method. J Eur Ceram Soc. 2017; 37(4): 1635-1642.
36. Abdellahi M, Najafinezhad A, Ghayour H, Saber-Samandari S, Khandan A. Preparing diopside nanoparticle scaffolds via space holder method: Simulation of the compressive strength and porosity. J Mech Behav Biomed Mater. 2017; 72: 171-181.
37. Karamian E, Nasehi A, Saber Samandari S, Khandan A. Fabrication of hydroxyapatite-baghdadite nanocomposite scaffolds coated by PCL/Bioglass with polyurethane polymeric sponge technique. Nmed J. 2017; 4(3): 177-183.
38. Sharafabadi AK, Abdellahi M, Kazemi A, Khandan A, Ozada N. A novel and economical route for synthesizing akermanite (Ca2MgSi2O7) nano-bioceramic. Mater Sci Eng C. 2017; 71: 1072-1078.
39. Sahmani S, Khandan A, Saber Samandari S, Aghdam MM. Nonlinear bending and instability analysis of bioceramics composed with magnetite nanoparticles: Fabrication, characterization, and simulation. Cer Int. 2018; 44(8); 9540-9549.
40. Saber Samandari S, Saber Samandari S. Biocompatible nanocomposite scaffolds based on copolymer-grafted chitosan for bone tissue engineering with drug delivery capability. Mater Sci Eng C. 2017; 75: 721-732.
41. Beladi F, Saber Samandari S, Saber Samandari S. Cellular compatibility of nanocomposite scaffolds based on hydroxyapatite entrapped in cellulose network for bone repair. Mater Sci Eng C. 2017; 75: 385-392.
42. Abd-Khorsand S, Saber Samandari S, Saber Samandari S. Development of nanocomposite scaffolds based on TiO2 doped in grafted chitosan/hydroxyapatite by freeze drying method and evaluation of biocompatibility. Int J Biol Macromol. 2017; 101: 51-58.
43. Heydary HA, Karamian E, Poorazizi E, Heydaripour J, Khandan A. Electrospun of polymer/bioceramic nanocomposite as a new soft tissue for biomedical applications. J Asian Ceram Soc. 2015; 3(4): 417-425.
44. Heydary HA, Karamian E, Poorazizi E, Khandan A, Heydaripour J. A novel nano-fiber of Iranian gum tragacanth-polyvinyl alcohol/nanoclay composite for wound healing applications. Proc Mat Sci. 11, 176-182.
45. Li C, Chou TW. Multiscale modeling of compressive behavior of carbon nanotube/polymer composites. Compos Sci Technol. 2006; 66(14): 2409-2414.
46. Aghadavoudi F, Golestanian H, Tadi Beni Y. Investigating the effects of resin crosslinking ratio on mechanical properties of epoxy-based nanocomposites using molecular dynamics. Polym Compos. 2017; 38(S1).
47. Aghadavoudi F, Golestanian H, Tadi Beni Y. Investigating the effects of CNT aspect ratio and agglomeration on elastic constants of crosslinked polymer nanocomposite using multiscale modeling. Poly Compo.
48. Moradi Dastjerdi R, Aghadavoudi F. Static analysis of functionally graded nanocomposite sandwich plates reinforced by defected CNT. Compos Struct. 2018; 5.
49. Saber Samandari S, Afaghi Khatibi A. The effect of interphase on the elastic modulus of polymer based nanocomposites. Key Eng Mater. 2006; 199-204.